This item is the archived peer-reviewed author-version of:

Iron(III) removal from acidic solutions using mesoporous titania microspheres prepared by vibrational droplet coagulation

IRON(III) REMOVAL FROM ACIDIC SOLUTIONS USING MESOPOROUS TITANIA MICROSPHERES PREPARED BY VIBRATIONAL DROPLET COAGULATION

Kenny Wyns[1], Nick Gys[1,2], Andrea Deibe Varela[1], Jeroen Spooren[1], Thomas Abo Atia[1,3], Elena M. Seftel[1] and Bart Michielsen[1,*]

[1]Unit Sustainable Materials, VITO, Boeretang 200, BE-2400 Mol, Belgium

[2] Laboratory of Adsorption and Catalysis (LADCA), Department of Chemistry, University of Antwerp, Wilrijk, Belgium

[3]Department of Chemistry, KU Leuven, Celestijnenlaan 200F, B-3001 Leuven, Belgium

Corresponding author: bart.michielsen@vito.be

ABSTRACT

The removal of contaminants, such as Fe(III) from acidic leachates, is often needed as its presence as a contaminant hinders the recovery of the desired metals. An inorganic adsorbent of interest for the removal of Fe(III) is titania due to its high specific surface area and good chemical stability. However, besides the material properties, also the macroscopic shape of the adsorbent is important for its implementation. In this study we have shaped monodisperse titania microspheres using vibrating nozzle technology. In a first step, a suspension containing titania nanopowder and sodium alginate is broken up into monodisperse droplets. The droplets are then solidified through ionotropic gelation of the alginate binder molecules with the calcium ions used as solidification species. The thermally treated microspheres had an average diameter 518 µm, a specific surface area 97 mm² g^{-1} and an average pore size of 19 nm. These titania microspheres were employed as an adsorbent to remove Fe(III) from acidic solutions (pH 2). A maximum adsorption capacity of 13.2 mg g^{-1} was found. A high selectivity (k$_D$ 449 mL g^{-1}) was observed towards Fe(III) removal in an acidic leachate originating from a spend automotive catalyst. The titania microspheres could be easily separated and regenerated using a 0,1 M EDTA solution which was demonstrated for up to 5 cycles.

HIGHLIGHTS

- Monodisperse titania microspheres were prepared with an average size of 500 µm

- The titania microspheres selectively remove Fe from a spend automotive catalyst leachate

- Regenerability for Fe removal was demonstrated up to 5 cycles

KEYWORDS

Mesoporous titania, microspheres, vibrational jet-break-up, alginate coagulation mechanism, Fe(III) removal

1. INTRODUCTION

Besides the desired metals liberated during leaching processes, also other metals are released which can hinder the further purification and recovery. Therefore the removal from leachates of co-concurring metals which complicates recovery processes afterwards is essential. One such problem metal is the Fe(III), which is present in leachates from automotive catalyst and electronic waste hindering the recovery of Pd and Pt. An often employed solution is to obtain selectivity in the separation and recovery process by synthesising novel solid phase extraction materials specific for Pd and Pt. [1-5] However, there is always the chance that a small fraction of the Fe is also adsorbent and will end up into the final purified solution.

Another strategy is to selectively remove the Fe from the leachate as a pre-processing step. For this, a solid phase extraction material with high affinity for Fe and a good acid resistance is needed. Preferably this material can also be regenerated and re-used multiple times. Some studies suggest that titania (TiO_2) can remove different metals from aqueous solutions including Fe even at low pH.[6-13]. Moreover, it is low-cost, easily recyclable, non-swellable material which exhibits a high chemical stability in a wide pH range.

Most of the reported studies dealing with titania-type materials focus on the synthesis or testing in powder form, often even as nano-particles,[14] which makes their handling difficult. The removal from a solution requires centrifugation or high pressure filtering. Also for their use in a column set-up this results in very high pressure drops and clogging. One strategy to overcome these limitations is to shape or granulate the titania powders into porous microspheres to facilitate their applicability. The use of microspheres will minimize the occurrence of preferential pathways in a column set-up, lower the pressure drop or hydraulic conductivity and will ease its handling and recovery at the end of the process.

A strategy often used is the entrapment of the porous inorganic powders in biopolymeric matrices.[14-21] Recently, May et al.[19] investigated the encapsulation of TiO_2 with different polymeric hydrogels such as alginate, chitosan or agarose. Despite some benefits, the properties of hybrid materials limit in some cases their applicability. Some of the limitations are low thermal stability, swelling, deformation at high pressure, degradation of the polymeric matrix and/or reduced activity or functionality.

For applications were these properties are an issue, it is of importance to synthesize pure titania microspheres. A method to prepare titania spheres was reported by Dwivedi et al.[22] and Wu et al. [13] who describe the shaping starting from the alginate hydrogel template. In short, they prepared calcium alginate hydrogel microspheres followed by the exchange the water with isopropanol to obtain a water-free alginate alcogel microspheres. These spheres are soaked into titanium isopropoxide and the titanium isopropoxide impregnated in the alginate microspheres is hydrolysed with water. The resulting spheres are dried and thermally treated to remove the alginate polymeric template and crystallize the inorganic titania precursor. As an impregnation step with titanium isopropoxide requires a water-free environment a significant amount of organic solvents is used.

Recently Yu et al. [23] described a novel solvent free approach with reduced number of process steps. In this method, the sodium alginate is dripped into a $Ti(SO_4)_2$ solution to obtain Ti-alginate hydrogel microspheres. The resulting spheres were dried and thermally treated to remove the alginate template and crystalline titania phase. However, this way only limited amount of Ti and relative large amounts of alginate are present in the wet microspheres. This results in significantly shrinkage during drying and calcination resulting in deformed microspheres.

In this study we investigate an alternative method to obtain titania microspheres starting from a non-porous titania nanopowder, similar to previous studies on alumina.[24-26] The titania particles are dispersed into an alginate solution which is dripped into a calcium solution to obtain titania loaded Ca-alginate hydrogel microspheres. In the last step, these spheres are dried and thermally treated. The

main novelty is that microspheres with a high titania/alginate ratio's can be obtained in a 1-step process with reduced shrinkage during thermal treatment, resulting in a more cost effective process. We show that these microspheres can easily be used as a selective and regenerable Fe(III) scavenger from acidic solutions. Their main advantage being, that they can easily be collected and re-used.

EXPERIMENTAL

Chemicals

Sodium alginate BR-W was obtained from Brace GmbH (Karlstein am Main, Germany). TiO_2 nanoparticles dispersed in water (30 wt% in H_2O, W2730X) were purchased from Evonik and calcium chloride dihydrate was purchased from VWR Chemicals (Leuven, Belgium). $FeCl_3$ (97%) and EDTA (99,3%) were obtained from Sigma-Aldrich® and VWR Chemicals respectively . In order to give the desired pH to the solutions NaOH pellets and HCl fuming 37% for analysis EMSURE® from Merck were used.

Equipment & Analysis

Synthesis of the titania microspheres

The formation of the titania microspheres was done using a Microspherisator M from Brace GmbH (Karlstein am Main, Germany) of which the schematic set-up is depicted in Figure 1. It is a pilot-scale device with a throughput of 0.1 - 10 L suspension per hour, depending on the nozzle size used.
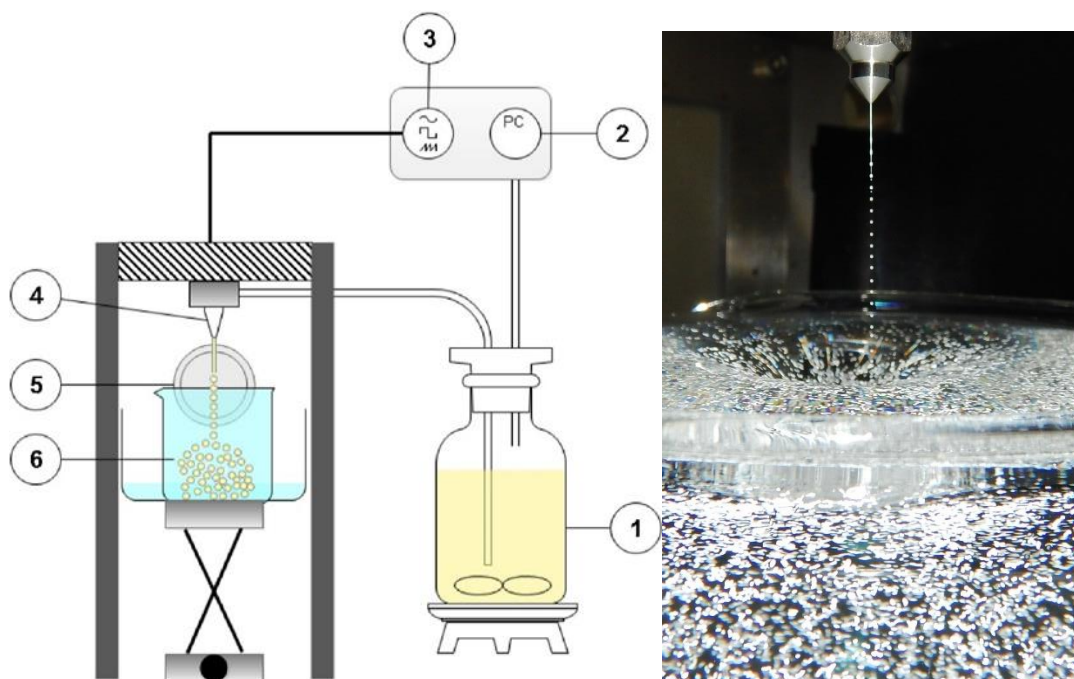
Figure 1: Schematic representation of the vibrational droplet coagulation set-up (taken from [24]) and image depicting the jet-break and coagulation in the CaCl₂ bath. (1) Feed vessel with magnetic stirrer; (2) Air pressure controller; (3) Vibration generator with frequency and amplitude control; (4) Nozzle; (5) Stroboscopic lamp; (6) Coagulation bath.

The procedure to prepare the titania microspheres was slightly modified as compared with the previously reported studies on alumina and silica microspheres.[24-27] In the first step a 4 wt% sodium-alginate aqueous solution was prepared by using a Eurostar 60 (IKA) type mixer. Then a mixture of the titania dispersion and distilled water was added, resulting in a suspension containing 20 wt% TiO_2 and 0.75 wt% alginate. This suspension was mixed for 60 min before use.

The prepared suspension was placed under pressure to obtain a liquid flow through a nozzle with a 300 µm orifice. It was determined that a flow rate of at least 5 mL min^{-1} was necessary to obtain a laminar jet. Once a laminar jet was obtained, the nozzle was vibrated by regulating the frequency and amplitude as such as a stable jet break-up of the suspension was produced. The fine control of the vibrating nozzle is of key importance when producing microspheres by this technology. A stable process results in uniform droplet sizes, a uniform distance between the droplets and no disturbing

movement of the droplets in the flow. Therefore, good visualisation of the jet-breakup is important. This is achieved by using a stroboscopic light that flashes in phase with the frequency applied to the nozzle. For the parameters described above, a stable jet-break up was observed in the frequency range of 240 and 400 Hz, while the amplitude was kept constant at 2000 mV.

The formed droplets fell into a coagulation bath containing a aqueous solution of $CaCl_2$. The divalent Ca^{2+} ions induced a rapid ionotropic gelation of the glucuronic acid block copolymers in the alginate resulting in a rigid structure. In this study different $CaCl_2$ concentrations (between 0.018 and 0.36 M) were used to study the effect on the properties of the obtained microspheres. The height of the coagulation bath was kept constant on the position of the first free droplet of the interrupted jet (around 2 cm).

The obtained microspheres were kept overnight in the coagulation bath to ensure a complete solidification of the structure. The wet microspheres were washed thoroughly with distilled water and soaked 3 times in 2-propanol, and subsequently dried overnight at 80 °C. In the next step, the samples were thermally treated at 500 °C for 2 hours (ramping rate of 2 °C min^{-1}) in order to remove the alginate content. Finally the samples were washed with 0,01 M HCl to remove the calcium ions present in the matrix.

The material properties of the samples were checked at different point in the synthesis process and the resulting codes are given in Table 1.

Table 1: Sample codes of the different prepared TiO₂ materials

MS	dried microspheres
CMS	microspheres calcined at 500°C
WCMS	calcined microspheres washed with 0.01 M HCl
FDP	powder resulting from the freeze drying of the W2730X precursor
CFDP	powder resulting from calcining FDP at 500 °C

Analysis methods

The dilute aqueous suspension was characterized in terms of particle size distribution by dynamic light scattering principle using a Zetasizer NanoZS (Malvern, UK) analyser. The particle size was measured to evaluate the agglomerate formations. Each sample was measured 3 times.

The rheology of the suspensions was measured with a Haake mars rheometer (Germany, cup Z43 DIN 53018 and rotor Z41 DIN 53018). Rheology curves were provided in a shear rate interval between 0.01 and 1000 s^{-1} and data points are collected when decreasing the shear rate. Viscosity screening in the shear rate interval took 5 min. The temperature was controlled by a thermostatic bath set at 25 °C.

Images of the obtained microspheres were acquired by optical microscopy using a ZeissDiscovery V12 stereomicroscope, equipped with a Plan Apo S 1.0xFWD 60 mm objective. Image collection was performed using an Axiovision MRc digital camera connected to the microscope. The surface of the microspheres was also investigated using a cold field emission scanning electron microscope (FEGSEM) of the type Nova Nano SEM 450 (FEI, USA) at 20 kV.

The particle size and shape parameters were determined via a combination of light diffraction and dynamic image analysis system (Microtrac S3500 with PartAn SI attachment). Each sample was measured for 30 s with the flow rate at 40 % of the maximum flow. From these measurements the

d_{10}, d_{50} and d_{90} values were derived, where the portion of microspheres with a diameter smaller than this value are respectively 10 %, 50 % and 90 %.

The feret ratio (L/W) is one of the most used shape factors in various applications to determine the sphericity of microspheres. It is determined as the ratio of the maximum (L) and minimum (W) feret diameter of the microspheres. Microspheres with feret ratio close to 1 are accepted as having a good sphericity, while higher values indicate a more elongated shape.[24, 28-30]

Thermogravimetric analysis (TGA) was performed on a STA 449C Jupiter (Netzsch, Germany) and performed in dry air (70 mL min^{-1}). The samples were heated from ambient temperature to 800 °C with a heating rate of 5 °C min^{-1}. The TGA equipment was coupled online to a mass spectrometer Omnistar GSD 301 O2 (Pfeiffer Vacuum, Germany) through a heat capillary (190 °C) measuring in the mass range of 12 -130 amu at a scan rate of 30 s per measurement.

The crystal phases of the titania microspheres were investigated by X-ray diffraction (XRD) on the powders obtained by milling the microspheres. The XRD spectra were recorded on a PANalytical X'Pert PRO MPD diffractometer with filtered Cu Kα radiation. Measurements were done in the 2θ mode using a bracket sample holder with a scanning speed of 0.04° per 4 s continuous mode. Rietveld analysis was applied to identify and quantify the crystal phases.

The surface area data were obtained on a Quantachrome Autosorb-iQ automated gas sorption analyser. Before analysis, the samples were outgassed under vacuum at 200 ºC for 24 h. Brunauer-Emmett-Teller (BET) method was used to calculate the surface area of the samples, in the p/p_0 range of 0.05-0.35. Pore size distribution was calculated using the Barrett-Joyner-Halenda (BJH) method, and the pore volume was measured at a relative pressure of 0.95.

In order to determine the calcium content of the titania spheres, the Inductively Coupled Plasma - Optical Emission Spectroscopy (ICP-OES) was used. For this, a total digestion of these solid samples was required. The measurement protocol is described in the supplementary information.

Fe(III) sorption experiments

Metal analysis

Metal concentration were determined by inductively coupled plasma optical emission spectroscopy (Agilent Technologies 5100). The system was equipped with a baffled cyclonic spray chamber and a Seaspray nebulizer was used for this purpose.

For the quantification of the elements, the ICP-AES was calibrated in 2% HNO_3 using several calibration solutions (until 2500 $\mu g\ L^{-1}$) in the axial viewing direction. Independent control samples were used to check the calibration, resulting in a recovery between 90-110%. Multiple emission lines were measured for all elements to verify possible interferences. All the samples were measured in different dilutions (from 5000 to 10 times) and two of the samples were spiked, the concentration of the spikes being half of the calibration concentration. When signal suppression of the internal standard (In or Lu) was more than 5%, the results were corrected. At the end of the analysis a remeasurement of the calibration blank and the highest calibration standard was performed. All calibration and control solutions used were made in the same 2% HNO_3 matrix as the diluted samples.

Synthetic solutions

The removal characteristics of Fe(III) acidic synthetic solutions were studied. To this end, the solutions were prepared using $FeCl_3$ and acidified using 0.1 M HCl. In all experiments 100 mg of the titania material was brought into contact with 10 mL of the synthetic solution and shaken at 100 rpm at 20°C. Afterwards, the aqueous phase was separated using a 0.45 µm cellulose filter (CHROMAFIL® RC-45/25 from MACHEREY-NAGEL GmbH & Co). The remaining Fe concentration in solution was determined using ICP-OES. To establish the kinetics a 200 mg L^{-1} Fe(III) solution was used and the contact time varied between 10 minutes and 24 hours. To establish the equilibrium isotherms the Fe(III) concentration was varied between 25 and 250 mg L^{-1} at a fixed contact time of 24 hours. All experiments were performed in duplicate.

The adsorption capacity q_i for these conditions can then be described by the following equation:

$$q_i = \frac{(C_0 - C_i)\, V}{m} \qquad \text{(equation 1)}$$

where C_0 and C_i are the initial and residual Fe(III) concentration in the aqueous phase, respectively. V is the volume of solution, and m is the weight of adsorbent.

Selectivity on automotive catalyst leachate

The selectivity towards Fe removal was tested on an acidic leachate from a spent automotive catalyst. For the preparation of the leachate, a microwave assisted leaching step was used which is described in detail elsewhere.[31] The pH of the leachate was adjusted to 2 using some solid NaOH and afterwards filtered over a 0.45 µm cellulose filter (CHROMAFIL® RC-45/25 from MACHEREY-NAGEL GmbH & Co). To gain some insights in the selectivity 10 mL of leachate was brought into contact with 100 mg of the WCMS for 1440 minutes after which the concentration was determined. From this the distribution coefficient was calculated according to following formula:

$$K_D = \frac{q_e}{C_e} \qquad \text{(equation 2)}$$

Regeneration of the titania microspheres

The regeneration potential was evaluated in a single adsorption-desorption cycle. For the adsorption step, 100 mg of sorbent was brought into contact with 10 mL of a 200 mg L^{-1} Fe(III) solution at pH 2 in a 25 mL glass vial and shaken for 120 min. A time of 120 min was selected after this period a significant amount (50 %) of Fe(III) was absorbed and permits the completion of a full adsorption -desorption cycle in a day. Next, the Fe(III) loaded adsorbents were stripped by adding 10 mL of 0.1 M EDTA for different time intervals. Then, the regenerated adsorbents were used again in a subsequent adsorption experiment. After each (de)sorption step, the adsorbents were washed three times with 10 mL water for 10 min.

The regeneration efficiency of the microspheres can then be expressed by the following equation:

$$R\% = \frac{q_{Fe,2}}{q_{Fe,i}} \qquad \text{(equation 3)}$$

Where $q_{Fe,i}$ is the sorption initial capacity and $q_{Fe,2}$ is the sorption capacity after the first stripping step.

3. RESULTS AND DISCUSSION

3.1 Synthesis of the titania microspheres

The size and shape of microspheres prepared using droplet coagulation can be controlled by both chemical and physical parameters. The first category includes the suspension characteristics, such as the solid content, particle size, alginate type and composition of the coagulation bath. Parameters of importance related to the second category are the nozzle size, flow rate of the suspension and the applied frequency.

Suspension characteristics

In this study we start from a commercial fumed titania dispersion in water stabilised with acetic acid. The titania content in the dispersion is about 30 wt% and the pH is close to neutral.

A critical parameter of the starting suspension is the maximum particle size. Very large particles or agglomerates can induce a blockage inside the nozzle, disrupting the process. To this end, the particle size distribution (PSD) of the diluted titania dispersion and the final alginate-containing suspension was measured using dynamic light scattering analysis and the resulting size distribution is depicted in Figure S1. For the titania dispersion, a peak maximum is observed at 150 nm for the particle diameter, which is larger as indicated by the supplier (< 100 nm). Larsen et al.[32] found a multimodal distribution for the same product with a peak at 28 nm for the presumably the primary particles and a large peak at 140 nm of formed agglomerates. In the diluted suspension containing

alginate the maximum is shifted towards 204 nm, indicative for the formation of larger agglomerates. However, their submicron size is still sufficiently small to avoid nozzle blockages.
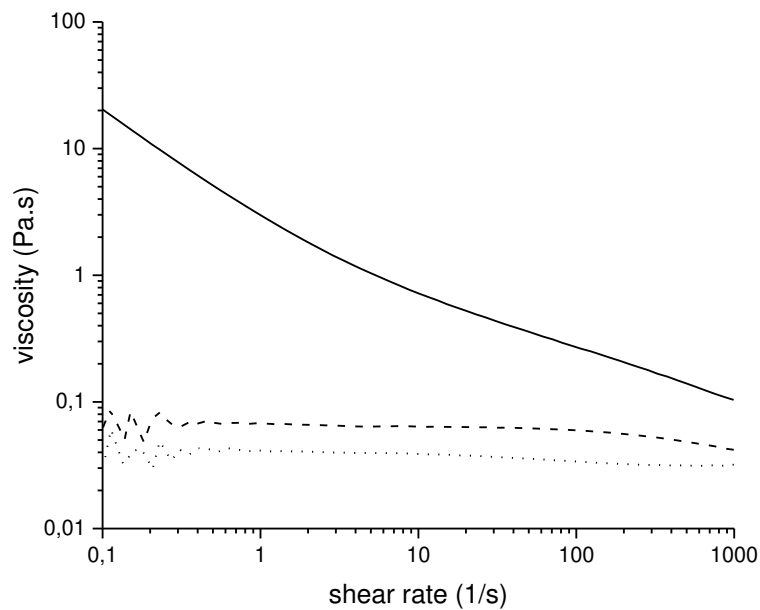

Figure 2: Viscosity curves of the titania-alginate suspension (solid line), a 30 wt% titania dispersion (dotted line) and a 1 wt% alginate solution (dashed line)

Another important parameter is the rheology of the suspension. The viscosity curves of the 30 wt% titania dispersion, a 1 wt% alginate solution and the alginate-titania suspension are given in Figure 2. Both the alginate solution as well as the titania suspension show a Newtonian behaviour and a viscosity value of 80 and 40 mPa s, respectively. However, when the two components are mixed together, the rheologic behaviour of the resulting suspension shows some significant differences. The behaviour of this suspension becomes shear-thinning and as a result, the viscosity curve shows a difference of two decades over the measured range. Also the viscosity values, even at high shears, are increased significantly. It should be mentioned that a high shear is encountered by the suspension at the nozzle level during the microsphere production process. The values for the viscosity at a shear of 100-1000 Hz are similar to previously reported studies focusing on processing of alumina[24] and silica containing suspensions[25], giving confidence that a jet-breakup of the suspension is possible.

Microsphere formation

In a first step the physical parameters for the suspension as described above were optimised for a nozzle of 300 µm. The laminar flow was obtained by fixing the flow rate at 5 mL min^{-1} to limit the impact of the droplets on the surface of the coagulation bath. Subsequently the frequency at which the nozzle vibrates was varied in order to determine the region in which a stable jet break-up is obtained. The lower limit of frequency resulting in a stable jet was found to be 240 Hz and the highest 400 Hz. Higher or lower frequencies resulted in disturbed jets leading to single droplets of different sizes and/or even droplets joined together, referred to by us as twins. The average d_a increases from around 450 µm up to 530 µm when the applied frequency is decreased (Table S1). The monodispersity (as indicated by the d_{90}/d_{10} ratio) is slightly decreased for the microspheres prepared at 400 Hz. This deviation is mainly due to the larger d_{90} indicating that a small fraction of larger microspheres is formed. This could indicate that some droplets collide upon impact and due to the smaller distance between the droplets and form a larger sphere in the coagulation bath. However, no difference was observed in the shape parameters. For the remainder of this study the frequency was fixed at 320 Hz.

Table 2: Size and shape parameters for the wet, dried and calcined microspheres prepared with a frequency of 320 Hz and a CaCl$_2$ concentration of 0.36 M. The last column gives the number of spheres measured to obtain the data.

	d$_{50}$ / µm	d$_a$ / µm	d$_{90}$/d$_{10}$	L/W	number of spheres
Wet	831	837 ± 30	1.09	1.14 ± 0.07	913
Dried	484	524 ± 42	1.16	1.2 ± 0.1	546
Calcined	513	518 ± 40	1.16	1.2 ± 0.1	419

The shape parameters of the microspheres prepared with this frequency are given Table 2 . The diameter of 837(30) µm observed for the prepared wet microspheres is larger than the size of the nozzle used. Upon drying they shrink by a factor of 38 % to 520(40) µm. After calcination at 500 °C the size and shape parameters do not change. This is different compared with the shaping of titania microspheres in other studies where the alginate is used as a template impregnated by titania precursors which shrink up to 75 % significantly after thermal treatment due to the low amount of Ti present [13, 22, 23]. The obtained spheres are monodisperse and the d_{90}/d_{10} ratio is close to 1. As can be observed in the optical images (Figure 3), the microspheres are not perfect spherical but have a slight oval shape. This is also indicated by the calculated feret ratio (L/W) values higher than 1 (Table 1). This slightly oval shape may be attributed to the flattening of the droplets upon impact with the coagulation bath. Afterwards the droplet relaxes and returns to its preferred spherical shape with the lowest surface tension. In previous research [25, 30, 33] it was found that the rapid coagulation of the alginate binder molecules with the Ca^{2+} ions may freeze the droplets in a shape not yet completely spherical. From the data in Table 3, it can be seen that by changing the concentration of the Ca^{2+} ions from 0.36 M to 0.036 M no improvement in both sphericity and L/W ratio can be observed.

Previous studies indicated that the Ca^{2+} concentration influences the shape of the obtained microspheres.[25, 30, 33] It was observed that high concentration of the Ca^{2+} leads to a tightening of the alginate gel network resulting in slightly smaller microspheres. However, the gelation mechanism at low concentrations is rather slow causing deformation and coalescence of the produced droplets.[25, 30, 33] Similar phenomena are observed for the titania microspheres prepared in this study. In Figure 3 images of the wet titania/alginate hydrogel microspheres prepared using different $CaCl_2$ concentrations (0.036 – 0.36 M) are depicted. Starting from a low concentration, e. g. of 0.036 M, several merged spheres are observed. It ranges from aggregates containing two spheres and a small neck at 0.036 M up to larger agglomerates containing up to 10 droplets at concentrations of 0.018 M Ca.
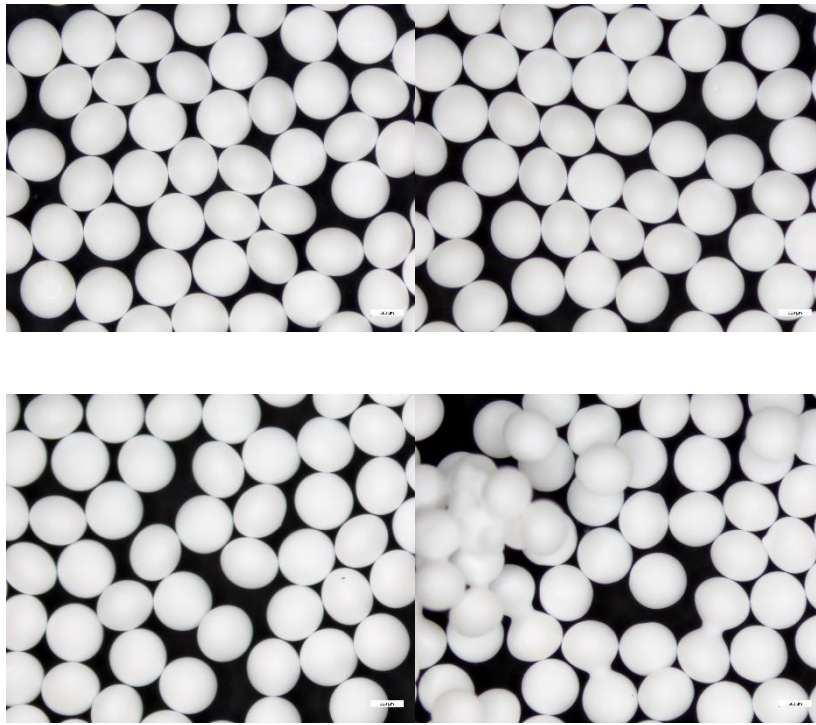
Figure 3: Image (20x magnification) of the wet microspheres prepared using a 300 μm nozzle at a frequency of 320 Hz but different concentrations of CaCl$_2$: 0.36 M (top left), 0.1 M (top right), 0.072 M (bottom left) and 0.036 M (bottom right)

The size and shape parameters of the dried alginate-titania spheres prepared using different concentrations ranging from 0.018 to 0.36 M are given in Table 3. The agglomerates were removed before measurement. A slight increase in the size of the microspheres (d_{50} and d_a) as a function of the CaCl$_2$ concentration is observed. The observed differences are small however and are within standard deviation of 40 μm as determined from the d_a. No impact is observed on the feret ratio or sphericity.

Table 3: Effect of the $CaCl_2$ concentration on the size and shape parameters for the dried microspheres. The last column gives the number of spheres measured to obtain the data.

Initial $CaCl_2$ concentration	d_{50}	d_{90}/d_{10}	L/W	#
0.360 M	484 µm	1.16	1.2 ± 0.1	959
0.100 M	487 µm	1.13	1.2 ± 0.1	669
0.072 M	489 µm	1.15	1.2 ± 0.1	845
0.036 M	516 µm	1.15	1.2 ± 0.1	148
0.018 M	504 µm	1.31	1.2 ± 0.1	665

Post-treatment

The thermal decomposition of the dried microspheres was investigated using TGA-MS and the resulting curves are shown in Figure 4. The TG curve can be divided into three stages. From room temperature up to 200 °C a weight loss of approximately 2 wt% is observed of which corresponds to the loss of physically bound water as indicated by the MS spectra. In the region between 200 and 500 °C an additional weight loss of 5 wt% is observed which can be attributed to the oxidative degradation of the calcium alginate matrix, such as decarboxylation reactions. This is corroborated by a signal in the mass ions assigned to the release of CO_2 (m/z = 44) and H_2O (m/z = 18). Above 500 °C no changes in mass are observed. Therefore this temperature was selected to perform the final thermal treatment, as it will result in titania microspheres having the highest specific surface which is important for the subsequent metal sorption. The details on the structural characteristics will be discussed in the next section.
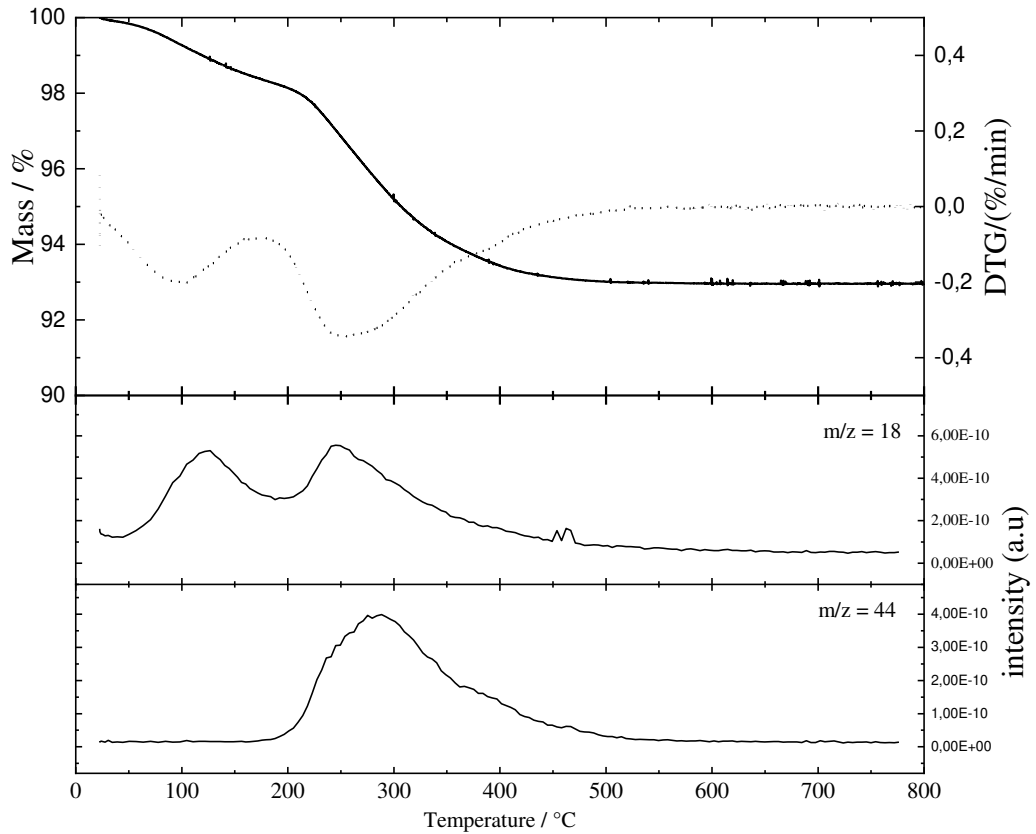
Figure 4: TG (full line) and DTG (dotted line) profile of the dried titania microspheres and profile of the mass ions 18 and 44 of the gaseous components (H_2O and CO_2) as function of temperature.

3.2 Characterisation of the titania microspheres

The phase composition and the crystallite size of the titania is important for their performance in subsequent applications. These characteristics were investigated using XRD analysis and the resulting diffraction patterns are shown in Figure 5. Rietveld refinement on the XRD patterns enabled the quantitative evaluation of the phases and the resulting data are given in Table 4. It may be concluded that the obtained calcined titania microspheres (CMS) contain mainly anatase phase with a small degree of rutile content, similar to the dried microspheres and the starting material. At increasing temperatures the anatase fraction transforms into rutile. The exact transformation temperature depends on particle size, atmosphere, surface area, heating rate and impurities.[34] Vargas et al. [35]

found that doping with different cations can influence the onset temperature of the anatase to rutile transformation and that calcium is an inhibitor. To study the effect of the calcium used during the shaping process a sample of the freeze dried W2730X dispersion (before calcination = FDP, after calcination CFDP) was treated in the same furnace run which led to an increased formation of rutile from 7.0 to 11.4 %. This indicates that the presence of the calcium ions in the structure have a inhibiting effect on the anatase to rutile transformation.
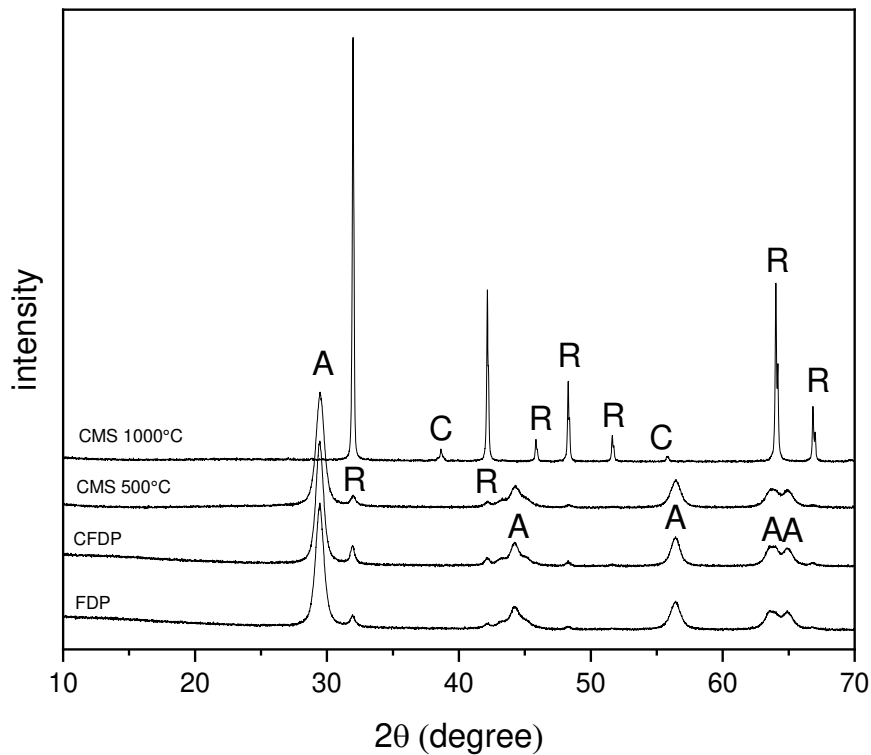

Figure 5: XRD patterns of the microspheres (top) calcined at 1000°C and 500°C and the starting material (bottom) as obtained after freeze drying without and with calcination at 500°C. A, R and C labels denote anatase, rutile and CaTiO₃ phases, respectively. The spectra are shifted for clarity.

The present study deals with the preparation of titania microspheres in the presence of calcium ions, therefore the solid state reaction between the titania phases and the calcium ions has to be taken into account. The content of calcium in the calcined microspheres was investigated using ICP-AES method. A calcium content of 8.0 ± 0.6 mg g^{-1} was found in the calcined titania microspheres, and this content showed to be similar for all the obtained microspheres, independent on the initial CaCl$_2$

concentration used. This may be attributed on the fact that during the microspheres production, the same alginate content is used in all cases, therefore a different Ca^{2+} concentration would not affect the overall Ca^{2+} loading into the produced microspheres. Furthermore, this is also an indication that all samples were properly washed as no residual physically adsorbed calcium is remaining and that all the measured calcium content is due to the incorporation in the alginate matrix.

Table 4: Distribution of the crystal phases in the starting material and microspheres, dried or calcined at different temperatures, together with their calculated crystallite size as determined by XRD analysis.

	Anatase		Rutile		CaTiO₃	
	wt%	Crystallite size (nm)	wt%	Crystallite size (nm)	wt%	Crystallite size (nm)
MS	91.5	12.8	8.5	23.5	-	-
CMS (500°C)	91.5	13.1	8.5	22.6	-	-
CMS (1000°C)	-	-	96.4	88	3.6	91
FDP	93.0	12.7	7.0	22.2	-	-
CFDP	88.6	14.3	11.4	26.5	-	-

Previously, during the preparation of alumina microspheres the formation of calcium hexa-aluminate was observed in the XRD spectra.[24] The presence of calcium titanate phases was not observed in the XRD spectra of the sample calcined at 500 °C. This may be attributed to the lower temperature of the thermal treatment used for the titania microspheres, e. g. 500 °C, as compared with the case of our previously studied alumina microspheres formation process. For the later, sintering

temperatures of up to 1650 °C were used, when formation of calcium hexa-aluminate phases was observed starting from 1000 °C.[24] Moreover, the formation of calcium titanates phases would be expected to occur at higher temperatures than 500°C as used in the present study, such as reported by Siriluk et al [36] for the solid state reaction type of mechanism. Generally reported, calcium titanates are obtained by solid state reactions at temperatures of 1000 °C or above.[37] Siriluk et al. [36] report temperatures for solid state reactions in the range of 1350 °C. The formation of calcium titanates at lower temperatures may be observed for other type of synthesis mechanisms, such as starting from reactive active compounds and/or using hydrothermal synthesis conditions[37], which is not the case in the present study. To further check this supposition, the XRD pattern of a thermally treated sample at 1000 °C was further analysed (pattern included in Figure 5). Accordingly, the formation of calcium titanate phase (approximately 3.6 wt%) is observed to be initiated by the solid state reaction between the Ca species and the titania phase. This would mean around 1 wt% of Ca is present which is in the same or of magnitude as the observed level of Ca from before and that all Ca is stoichiometrically converted into calcium titanate. Therefore, we may conclude that the formation of anatase microspheres with minor rutile phase are formed, with no other crystalline impurities are obtained using the present reported method and thermal treatment at 500°C.

Depending on the final application this amount of calcium can be either an advantage or a disadvantage. For example, Akpan et al. found that the photocatalytic activity of TiO_2 was enhanced by doping with 0.3-1 wt% of calcium ions.[38] However, in some other applications this might be undesirable. In order to reduce the amount of calcium content, the calcined microspheres were washed with a diluted hydrochloric acid solution, similar to the work reported by Mariott et al. [39] for carbon microspheres prepared from alginate. For these experiments, the calcined microspheres were soaked three times for 30 minutes in a 0.1 M hydrochloric acid solution, washed with deionized water and dried before further analysis. By this procedure, the calcium content could be reduced with a factor

of 3, namely to 2.7 ± 0.1 mg g^{-1} as measured by ICP-AES analysis. The code used for the resulting spheres is WCMS.

Figure 6 shows the SEM images of the surface of a calcined microsphere before and after the washing with HCl. A clear effect of the treatment on the surface of the microsphere can be observed. After the treatment the surface contains small holes of a size between 2 and 5 µm in diameter.
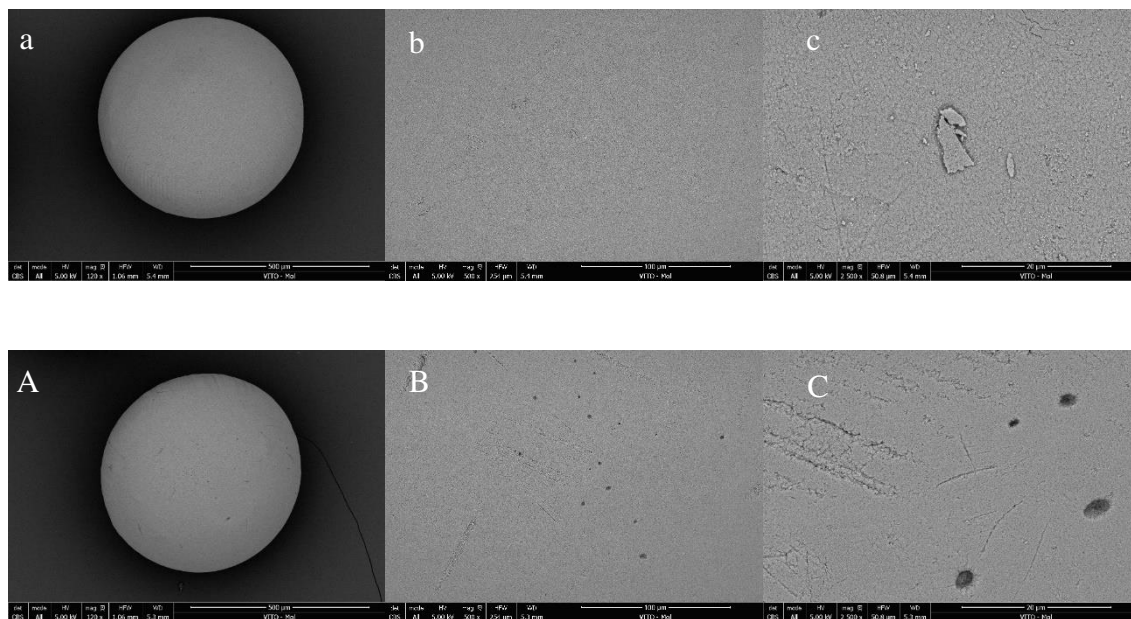

Figure 6: SEM images of the CMS (top) and the WCMS (bottom): 120x (a,A), 500x(b,B) and 2500x (c,C).

Further, the porosity of the obtained titania microspheres was investigated using nitrogen physisorption measurements. The standard Brunauer-Emmett-Teller (BET) method was used to calculate the specific surface area. The pore size distribution was determined using the Barrett-Joyner-Halenda (BJH) analysis of the N_2 adsorption/desorption isotherms (Figure 7).
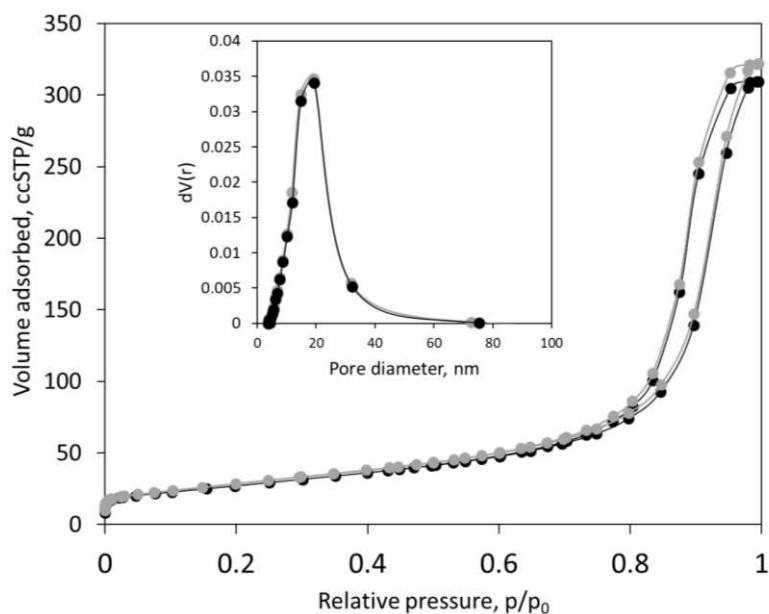
Figure 7. N$_2$ adsorption/desorption isotherms and BJH pore size distribution (inserted graph) of the CMS before (black curves) and WCMS (grey curves).

The shape of the curves is typical for a Type IV isotherm, with a small plateau at high relative pressures, characteristic of mesoporous materials. The H$_1$ hysteresis loop (originally known as Type A) has a fairly narrow loop with nearly parallel adsorption and desorption branches. The microspheres contain mesopores arising from the aggregation of the nanoparticles. The H$_1$-like hysteresis is usually explained by the presence of agglomerates defined as rigidly joined particles.[40] These isotherms are now termed Type IVa. The main adsorption occur at high relative pressures, e. g. above p/p$_0$ of 0.8, indicating the presence of large mesopores, which is also confirmed by the BJH analysis. Consequently, an average pore diameter of ~19 nm is recorded. The shape of both isotherms and pore size distributions indicate no obvious changes during to the HCl washing step.

Table 5: Specific surface area (BET), pore size and pore volume (BJH) of the calcined titania microspheres prepared using 0.1 and 0.36 M CaCl$_2$ concentrations. Values from other studies are given as well.

	SSA (m^2 g^{-1})	Pore diameter (nm)	Pore volume (cm^3 g^{-1})	Reference
CMS	97 ± 4	19 ±1	0.48 ± 0.07	-
WCMS	97 ±6	19 ± 1	0.48 ± 0.05	-
Charu et al.	67	19.8	0.33	[22]
Wu et al.	144	2 - 6	-	[13]
Yu et al.	29 – 57	15.5 - 37.8	0.21-0.5	[23]

The resulting values for the calcined microspheres prepared before and after the treatment with HCl are summarized in Table 5, together with values from previous studies. For all the obtained microspheres, a relatively high specific surface area of ~97 m^2 g^{-1} was obtained. Furthermore, it may be observed that the pore diameter is not significantly influenced by the initial CaCl$_2$ concentration or the washing with hydrochloric acid. The effect of the initial CaCl$_2$ concentration is summarized in the supplementary data (Table S2). If we compare the data obtained in this study with titania microspheres prepared in previous studies using alginate impregnation with titanium organic precursors, we may conclude that 30-40 % higher specific surface area is obtained as compared to samples with a similar pore diameter of 16-20 nm. Wu et al. reported higher specific surface area values, however their material is characterized by much smaller the pore diameter of, e. g. 2-6 nm as compared to 17-19 nm reported in the present study.

3.3 Removal of Fe(III) ions

The Fe(III) removal performance from acidic solutions was tested for the FDP, CFDP and the WCMS sample. The CMS was not taken into consideration as the pH of the synthetic solutions and leachate employed is equal to that of the washing solution. As the release of the Ca into the eluate is not desired this sample was omitted from the assessment.

Fe removal selectivity from a spend automotive catalyst leachate

The selectivity towards metal removal of the WCMS was tested on a leachate from spent automotive catalyst in order to test the selectivity of the metal removal under realistic conditions. This leachate contains a multitude of metals in various concentration at pH 2. The parameters important for the separation performance are given in Table 6. As during the acidic leaching with 6 M HCl also an oxidising agent H_2O_2 ((10% v/v) is used the dominant iron species will be Fe(III). [31]

As can be from these the Fe is very selectively removed from the leachate by the WCMS with a very high K_d value of 450 mL g^{-1}. There is also some selectively towards Ti ($K_d = 14$ mL g^{-1}) and Cr ($K_d = 11$ mL g^{-1}) and almost none to the other metals ($K_d < 10$ mL g^{-1}) present in the leachate. This indicated that the solid phase extraction of the Fe by prepared titania microspheres is an excellent pre-treatment step for the further purification of the leachate. Especially the separation factor of the Fe over the Pd is very high (3367) as almost none of the Pd is adsorbed by the WCMS. Still some Ca is removed from the microspheres resulting in an increased concentration and a negative K_d and separation factor. It is expected that over the course of consecutive cycles this phenomena will decrease and the release of Ca will stop.

Table 6: Metal concentration in the leachate of a spend automotive catalyst (C_0), after adsorption by WCMS (C_e), the distribution coefficient of the metals and the separation factor of Fe over the metal. The standard deviation is based on 2 separate experiments.

	C_0 (mg L^{-1})	C_e (mg L^{-1})	K_d (mL g^{-1})	α^{Fe}_M
Al	12350 ± 70	11800 ± 70	1.9	241
Ce	2655 ± 21	2580 ± 21	1.2	386
Ba	442 ± 1	442 ± 1	0.0	-
La	207 ± 1	207 ± 1	0.0	-
Fe	176.0 ± 0.3	14.4 ± 0.3	448.9	-
Pt	175 ± 1	170 ± 1	1.2	382
Pd	151 ± 1	150 ± 1	0.1	3367
Ca	43.1 ± 0.1	193.0 ± 0.1	-31.1	-14.4
Y	42.1 ± 0.1	41.4 ± 0.1	0.7	664
Nd	39.5 ± 0.1	38.5 ± 0.1	1.1	411
Ti	30.1 ± 0.1	22.4 ± 0.4	13.8	32.6
Cr	16.1 ± 0.1	12.7 ± 0.1	10.9	41.1
Rh	8.1 ± 0.2	8.0 ± 0.1	0.8	596
Cu	2.16 ± 0.01	1.92 ± 0.02	5.1	88

Fe(III) removal capacity

Besides selectively another important aspect is the maximum capacity. This can be determined the Fe(III) sorption isotherm which is derived from bringing the titania materials into contact solutions containing different concentrations and measure the Fe(III) concentration at equilibrium (24 hours).[41, 42] The experimental equilibrium data obtained this way was evaluated using the ISOFIT

software.[43] Both the Langmuir (equation 4) and Freundlich (equation 5) isotherm models were

explored which are given by the following formula's respectively:

$$q_e = \frac{Q_{max}K_LC_e}{(1+K_LC_e)}$$ (equation 4)

$$q_e = K_FC_e^{\frac{1}{n}}$$ (equation 5)

Hereby C_e (mg L^{-1}) is the concentration of Fe(III) in solution at equilibrium, Q_{max} (mg g^{-1}) is the

maximum adsorption capacity based on the Langmuir equation, K_L (L mg^{-1}) is the Langmuir constant,

K_F is the adsorption coefficient and 1/n is the adsorption intensity based on the Freundlich equation.
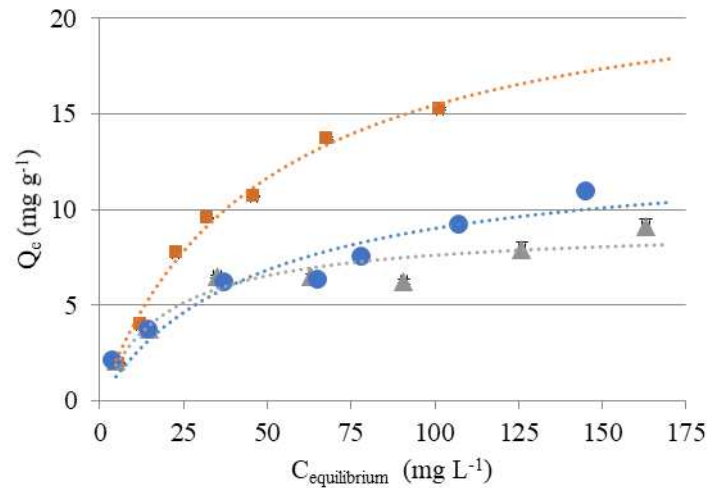

Figure 8: Effect of concentration (1440 min contact time) on the uptake of Fe(III) ions for the FDP (orange squares), CFDP (grey

triangles), and the WCMS (blue circles). The dotted lines are the plotted isotherms obtained using the Freundlich model.

The resulting values for FDP, CFDP and WCMS are gives in Table 7 and the modeled Freundlich

isotherm is plotted in Figure 8. From these data it can be observed that the calcination step has the

largest influence. The maximum adsorption capacity of the powder halves from 23 mg g^{-1} (CFP) to

13 mg g^{-1} (CFDP) after this step. The value for the microspheres is similar to that of the calcined

powder.

	Langmuir			Freundlich		
	Q_{max} (mg g^{-1})	K_L (L mg^{-1})	R^2	n	K_f	R^2
FDP	22.99	0.0021	0.991	1.80	1.24	0.961
CFDP	9.07	0.0051	0.905	2.93	1.54	0.911
WCMS	13.24	0.0021	0.927	2.17	1.07	0.971

Fe(III) removal kinetics

The effect of the contact time on the Fe(III) removal from a 200 mg L^{-1} solution for both the CFDP and the WCMS and the resulting capacity q_t is given in Figure 9. The powder (CFDP) shows a fast initial uptake of 70 % Fe(III) within the first 30 minutes followed by a slower uptake in the next 90 minutes. The Fe(III) removal of the microspheres (WCMS) was slower having only a 20 % uptake in the first 30 minutes which continues to slowly increase over time. This indicates that some diffusion limitations are present in the microspheres (WCMS, d_{50} = 450 µm) compared to the powder (CFDP, d_{50} = 2 µm), hindering the uptake over time. While the slower kinetics are not preferred, it does not necessary hinder the application. The selectivity and the easy and safe recovery of the sorbent are more important than the kinetics. Also, in a column type of application the solution will be forced more into the pores decreasing surface limitations.

The experimental data were evaluated using the non-linear form of the pseudo-first order (PFO) kinetic model (Eq. 8) and pseudo-second order (PSO) kinetic model (Eq. 9):

$$q_t = q_e(1 - exp^{-k_1 t}) \quad \text{(equation 8)}$$

$$q_t = \frac{k_2 q_e^2 t}{1 + k_2 q_e t} \quad \text{(equation 9)}$$

In which q_e is the adsorbed amount of Fe(III) (mg g^{-1}) at equilibrium, q_t is the uptake at any time t (mg g^{-1}), k_1 is pseudo-first order (min^{-1}) rate constant and the k_2 is the pseudo-second order (g mg^{-1} min^{-1}) rate constant, respectively.[42] The modeled curve is also shown in Figure 9 and the resulting values are given in Table 8. The best fit is obtained using the PSO model, indicating that the main adsorption mechanism is chemisorption. The slower uptake of the Fe(III) is also visible from the rate constant, as this is more than 10 times smaller for WCMS.
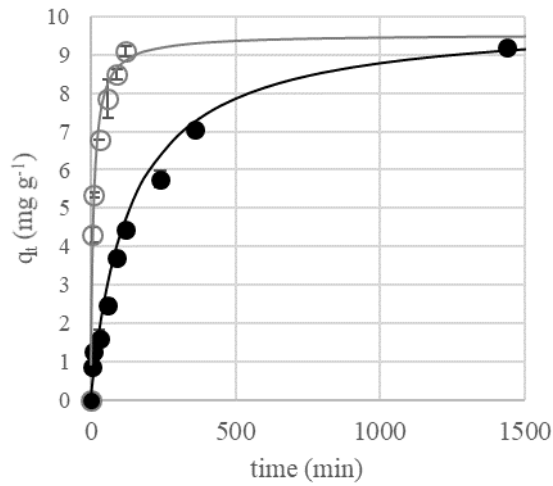

Figure 9: Adsorption capacity as a function of time (q_t) for the removal of Fe(III) on CFDP (open circles) and WCMS (full circles) and the modelled trend according to the pseudo second-order model.

Table 8: Kinetic parameters fitted using the PFO and PSO model for Fe(III) adsorption on CFDP and WCMS.

	experiment	PFO			PSO		
	$q_{e,,exp}$ (mg Fe g^{-1})	$q_{e,cal}$ (mg Fe g^{-1})	k_1 (min^{-1})	R^2	$q_{e,cal}$ (mg Fe g^{-1})	k_2 (g mg^{-1} min^{-1})	R^2
CFDP	9.60	6.13	0.0267	0.9363	9.99	0.0120	0.9957
WCMS	9.75	8.58	0.0053	0.9391	10.38	0.0009	0.9917

Regeneration of the WCMS

Due to their size the recovery of the microspheres is easy and fast by either decantation of using a filter with large mesh size. For practical application the metal scavenger are preferably regenerated and re-used. To this end, Fe(III) from loaded microspheres beads was stripped using 0.1 M EDTA. It was found that 77 ± 4 % of the initial Fe(III) capacity was available after 10 minutes exposure to the stripping solution which increased to 81 ± 2 % after 30 minutes and 90 ± 4 % after 2 hours.
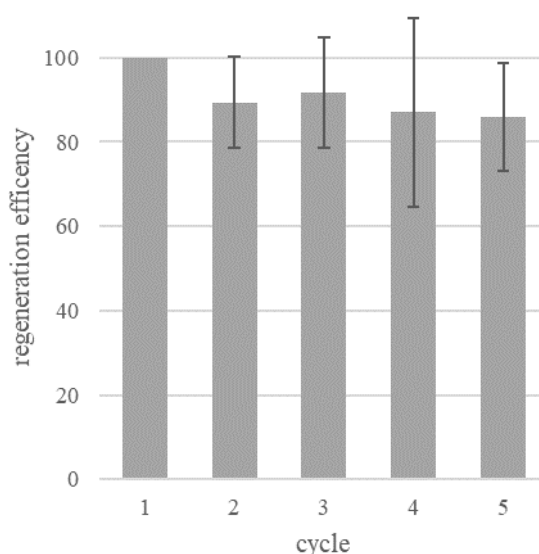

Figure 10: Adsorption capacity of the titania beads for 5 successive regeneration cycles with 0.1 M EDTA. The initial Fe(III) ions concentration was 200 mg L^{-1}, the L/S ratio 1000 and the contact time was 2 h for each cycle. The experiment was performed in duplicate and the resulting standard deviation (95 % confidence interval) is shown by the depicted error bars..

We used WCMS to remove Fe(III) from a 200 mg L^{-1} synthetic solution during five consecutive adsorption-desorption cycles using 0,1 M EDTA (Figure 10). The capacity seems to decrease slightly from the first towards the fifth cycle. However, the variation in capacity between the cycles is still within the experimental error. This results show that the titania microspheres can be easily regenerated and used for multiple times without a significant loss in performance. The resulting Fe-EDTA can then be precipitated and the iron oxide can be recovered after calcination.

4. CONCLUSIONS

This study reports a facile method to prepare monodisperse titania microspheres by using vibrational droplet coagulation technology. The physical parameters, such as the frequency and amplitude applied at the nozzle level, were optimized in order to control the size of the produced droplets. This resulted in monodisperse microspheres with high degree of sphericity. After the removal of the alginate matrix by thermal treatment at 500 °C, a specific surface area of 97 m² g^{-1} was found with pores in the mesoporous range due to the powder packing. The residual Ca could be partially removed by washing with HCl, reducing the amount by a factor of 67 %. These titania microspheres could be employed as a adsorbent to remove Fe(III) from acidic solutions and a high selectivity was observed in an leachate from a spend automotive catalyst. The titania microspheres could be easily separated and regenerated using a 0,1 M EDTA solution which was demonstrated for up to 5 cycles.

REFERENCES

[1] Q.A. Trieu, S. Pellet-Rostaing, G. Arrachart, Y. Traore, S. Kimbel, S. Daniele, Interfacial study of surface-modified ZrO2 nanoparticles with thioctic acid for the selective recovery of palladium and gold from electronic industrial wastewater, Separation and Purification Technology 237 (2020) 116353.

[2] F. Bai, G. Ye, G. Chen, J. Wei, J. Wang, J. Chen, Highly selective recovery of palladium by a new silica-based adsorbent functionalized with macrocyclic ligand, Separation and Purification Technology 106 (2013) 38-46.

[3] F. Xie, R. Fan, Q. Yi, Z. Fan, Q. Zhang, Z. Luo, Adsorption recovery of Pd(II) from aqueous solutions by persimmon residual based bio-sorbent, Hydrometallurgy 165 (2016) 323-328.

[4] O. Lanaridi, A.R. Sahoo, A. Limbeck, S. Naghdi, D. Eder, E. Eitenberger, Z. Csendes, M. Schnürch, K. Bica-Schröder, Toward the Recovery of Platinum Group Metals from a Spent Automotive Catalyst with Supported Ionic Liquid Phases, ACS Sustainable Chemistry & Engineering 9(1) (2021) 375-386.

[5] E. Lahtinen, M.M. Hänninen, K. Kinnunen, H.M. Tuononen, A. Väisänen, K. Rissanen, M. Haukka, Porous 3D Printed Scavenger Filters for Selective Recovery of Precious Metals from Electronic Waste, Advanced Sustainable Systems 2(10) (2018) 1800048.

[6] H. Gomaa, M.A. Shenashen, H. Yamaguchi, A.S. Alamoudi, M. Abdelmottaleb, M.F. Cheira, T.A. Seaf El-Naser, S.A. El-Safty, Highly-efficient removal of AsV, Pb2+, Fe3+, and Al3+ pollutants from water using hierarchical, microscopic TiO2 and TiOF2 adsorbents through batch and fixed-bed columnar techniques, Journal of Cleaner Production 182 (2018) 910-925.

[7] D.E. Tsydenov, A.A. Shutilov, G.A. Zenkovets, A.V. Vorontsov, Hydrous TiO2 materials and their application for sorption of inorganic ions, Chemical Engineering Journal 251 (2014) 131-137.

[8] C.R. Quétel, E. Vassileva, I. Petrov, K. Chakarova, K.I. Hadjiivanov, First results on Fe solid-phase extraction from coastal seawater using anatase TiO2 nano-particles, Analytical and Bioanalytical Chemistry 396(6) (2010) 2349-2361.

[9] S. Bang, M. Patel, L. Lippincott, X. Meng, Removal of arsenic from groundwater by granular titanium dioxide adsorbent, Chemosphere 60(3) (2005) 389-397.

[10] D.S. Han, A. Abdel-Wahab, B. Batchelor, Surface complexation modeling of arsenic(III) and arsenic(V) adsorption onto nanoporous titania adsorbents (NTAs), Journal of Colloid and Interface Science 348(2) (2010) 591-599.

[11] N.N. Gracheva, A.Y. Romanchuk, E.A. Smirnov, M.A. Meledina, A.V. Garshev, E.A. Shirshin, V.V. Fadeev, S.N. Kalmykov, Am(III) sorption onto TiO2 samples with different crystallinity and varying pore size distributions, Applied Geochemistry 42 (2014) 69-76.

[12] L. Yan, Y. Huang, J. Cui, C. Jing, Simultaneous As(III) and Cd removal from copper smelting wastewater using granular TiO2 columns, Water Research 68 (2015) 572-579.

[13] N. Wu, H. Wei, L. Zhang, Efficient Removal of Heavy Metal Ions with Biopolymer Template Synthesized Mesoporous Titania Beads of Hundreds of Micrometers Size, Environmental Science & Technology 46(1) (2012) 419-425.

[14] J. Gjipalaj, I. Alessandri, Easy recovery, mechanical stability, enhanced adsorption capacity and recyclability of alginate-based TiO2 macrobead photocatalysts for water treatment, Journal of Environmental Chemical Engineering 5(2) (2017) 1763-1770.

[15] M.H. Farzana, S. Meenakshi, Photo-decolorization and detoxification of toxic dyes using titanium dioxide impregnated chitosan beads, International Journal of Biological Macromolecules 70 (2014) 420-426.

[16] S. Thakur, S. Pandey, O.A. Arotiba, Development of a sodium alginate-based organic/inorganic superabsorbent composite hydrogel for adsorption of methylene blue, Carbohydrate Polymers 153 (2016) 34-46.

[17] J.Q. Albarelli, D.T. Santos, S. Murphy, M. Oelgemöller, Use of Ca–alginate as a novel support for TiO2 immobilization in methylene blue decolorisation, Water Science and Technology 60(4) (2009) 1081-1087.

[18] D. Kanakaraju, N. Shahdad, Y.C. Lim, A. Pace, Magnetic hybrid TiO2/Alg/FeNPs triads for the efficient removal of methylene blue from water, Sustainable Chemistry and Pharmacy 8 (2018) 50-62.

[19] N.X.D. Mai, D. Park, J. Yoon, J. Hur, Comparative Study of Hydrogel-Based Recyclable Photocatalysts, Journal of Nanoscience and Nanotechnology 18(2) (2018) 1361-1364.

[20] D. Kanakaraju, S. Ravichandar, Y.C. Lim, Combined effects of adsorption and photocatalysis by hybrid TiO2/ZnO-calcium alginate beads for the removal of copper, Journal of Environmental Sciences 55 (2017) 214-223.

[21] N.X.D. Mai, J. Bae, I.T. Kim, S.H. Park, G.W. Lee, J.H. Kim, D. Lee, H. Bin Son, Y.C. Lee, J. Hur, A recyclable, recoverable, and reformable hydrogel-based smart photocatalyst, Environ.-Sci. Nano 4(4) (2017) 955-966.

[22] C. Dwivedi, N. Raje, J. Nuwad, M. Kumar, P.N. Bajaj, Synthesis and characterization of mesoporous titania microspheres and their applications, Chemical Engineering Journal 193-194 (2012) 178-186.

[23] C. Yu, X. Li, Z. Liu, X. Yang, Y. Huang, J. Lin, J. Zhang, C. Tang, Synthesis of hierarchically porous TiO2 nanomaterials using alginate as soft templates, Materials Research Bulletin 83 (2016) 609-614.

[24] J. Pype, B. Michielsen, E.M. Seftel, S. Mullens, V. Meynen, Development of alumina microspheres with controlled size and shape by vibrational droplet coagulation, Journal of the European Ceramic Society 37(1) (2017) 189-198.

[25] J. Roosen, J. Pype, K. Binnemans, S. Mullens, Shaping of Alginate–Silica Hybrid Materials into Microspheres through Vibrating-Nozzle Technology and Their Use for the Recovery of Neodymium from Aqueous Solutions, Industrial & Engineering Chemistry Research 54(51) (2015) 12836-12846.

[26] J. Pype, B. Michielsen, S. Mullens, V. Meynen, Versatile use of droplet coagulation: Shaping fine-grained SiO2 and Al2O3 waste streams into monodisperse microspheres, Sustainable Materials and Technologies 14 (2017) 19-28.

[27] J. Pype, B. Michielsen, S. Mullens, V. Meynen, Impact of inorganic waste fines on structure of mullite microspheres by reaction sintering, Journal of the European Ceramic Society 38(6) (2018) 2612-2620.

[28] D. Wilkinson, K. Patchigolla, Comparison of Particle Size Distributions Measured Using Different Techniques AU - Li, M, Particulate Science and Technology 23(3) (2005) 265-284.

[29] D.O.C. Souza, F.C. Menegalli, Image analysis: Statistical study of particle size distribution and shape characterization, Powder Technology 214(1) (2011) 57-63.

[30] B.-B. Lee, P. Ravindra, E.-S. Chan, Size and Shape of Calcium Alginate Beads Produced by Extrusion Dripping, Chemical Engineering & Technology 36(10) (2013) 1627-1642.

[31] T. Abo Atia, W. Wouters, G. Monforte, J. Spooren, Microwave chloride leaching of valuable elements from spent automotive catalysts: Understanding the role of hydrogen peroxide, Resources, Conservation and Recycling 166 (2021) 105349.

[32] S.T. Larsen, M. Roursgaard, K.A. Jensen, G.D. Nielsen, Nano Titanium Dioxide Particles Promote Allergic Sensitization and Lung Inflammation in Mice, Basic & Clinical Pharmacology & Toxicology 106(2) (2010) 114-117.

[33] A. Islam, Y.H. Taufiq-Yap, P. Ravindra, M. Moniruzzaman, E.-S. Chan, Development of a procedure for spherical alginate–boehmite particle preparation, Advanced Powder Technology 24(6) (2013) 1119-1125.

[34] D.A.H. Hanaor, C.C. Sorrell, Review of the anatase to rutile phase transformation, Journal of Materials Science 46(4) (2011) 855-874.

[35] S. Vargas, R. Arroyo, E. Haro, R. Rodríguez, Effects of cationic dopants on the phase transition temperature of titania prepared by the sol-gel method, Journal of Materials Research 14(10) (1999) 3932-3937.

[36] S. Cherdchom, T. Rattanaphan, T. Chanadee, Calcium Titanate from Food Waste: Combustion Synthesis, Sintering, Characterization, and Properties, Advances in Materials Science and Engineering 2019 (2019) 9639016.

[37] G. Pfaff, Synthesis of calcium titanate powders by the sol-gel process, Chemistry of Materials 6(1) (1994) 58-62.

[38] U.G. Akpan, B. Hameed, Enhancement of the Photocatalytic Activity of TiO2 by Doping it with Calcium Ions, Journal of colloid and interface science 357 (2011) 168-78.

[39] A. Marriott, E. Bergström, A. Hunt, J. Thomas-Oates, J. Clark, A natural template approach to mesoporous carbon spheres for use as green chromatographic stationary phases, RSC Advances 4 (2013) 222.

[40] F. Rouquerol, J. Rouquerol, K. Sing, CHAPTER 13 - General Conclusions and Recommendations, in: F. Rouquerol, J. Rouquerol, K. Sing (Eds.), Adsorption by Powders and Porous Solids, Academic Press, London, 1999, pp. 439-447.

[41] H.N. Tran, S.-J. You, A. Hosseini-Bandegharaei, H.-P. Chao, Mistakes and inconsistencies regarding adsorption of contaminants from aqueous solutions: A critical review, Water Research 120 (2017) 88-116.

[42] M. Ateia, D.E. Helbling, W.R. Dichtel, Best Practices for Evaluating New Materials as Adsorbents for Water Treatment, ACS Materials Letters 2(11) (2020) 1532-1544.

[43] L.S. Matott, A.J. Rabideau, ISOFIT – A program for fitting sorption isotherms to experimental data, Environmental Modelling & Software 23(5) (2008) 670-676.